This article was downloaded by:
On: *19 January 2011*
Access details: *Access Details: Free Access*
Publisher *Taylor & Francis*
Informa Ltd Registered in England and Wales Registered Number: 1072954 Registered office: Mortimer House, 37-41 Mortimer Street, London W1T 3JH, UK

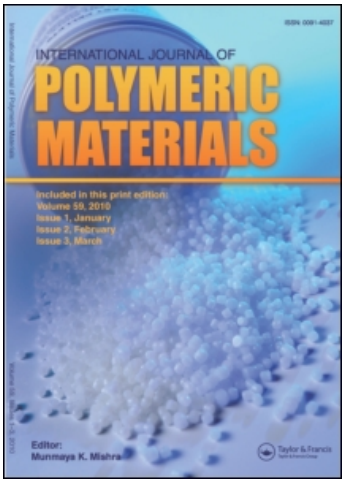


**International Journal of Polymeric Materials**
Publication details, including instructions for authors and subscription information:
http://www.informaworld.com/smpp/title~content=t713647664

# Order in the amorphous state of poly(ethylene terephthalate) as revealed by microhardness: Creep behavior and physical aging

D. R. Rueda[a]; M. C. García Gutiérrez[a]; F. J. Baltá Calleja[a]; S. Piccarolo[b]
[a] Instituto de Estructura de la Materia, CSIC, Madrid, Spain [b] Dipartimento di Ingegneria Chimica dei Processi e dei Materiali, Univeristà di Palermo, Palermo, Italy

Online publication date: 27 October 2010

**To cite this Article** Rueda, D. R. , Gutiérrez, M. C. García , Calleja, F. J. Baltá and Piccarolo, S.(2002) 'Order in the amorphous state of poly(ethylene terephthalate) as revealed by microhardness: Creep behavior and physical aging', International Journal of Polymeric Materials, 51: 10, 897 — 908
**To link to this Article: DOI:** 10.1080/714975674
**URL:** http://dx.doi.org/10.1080/714975674

PLEASE SCROLL DOWN FOR ARTICLE

Full terms and conditions of use: http://www.informaworld.com/terms-and-conditions-of-access.pdf

This article may be used for research, teaching and private study purposes. Any substantial or systematic reproduction, re-distribution, re-selling, loan or sub-licensing, systematic supply or distribution in any form to anyone is expressly forbidden.

The publisher does not give any warranty express or implied or make any representation that the contents will be complete or accurate or up to date. The accuracy of any instructions, formulae and drug doses should be independently verified with primary sources. The publisher shall not be liable for any loss, actions, claims, proceedings, demand or costs or damages whatsoever or howsoever caused arising directly or indirectly in connection with or arising out of the use of this material.

*International Journal of Polymeric Materials*, 51:897–908, 2002
Copyright © 2002 Taylor and Francis
0091-4037/02 $12.00 + .00
DOI: 10.1080/00914030290046417

Downloaded At: 09:52 19 January 2011

# ORDER IN THE AMORPHOUS STATE OF POLY(ETHYLENE TEREPHTHALATE) AS REVEALED BY MICROHARDNESS: CREEP BEHAVIOR AND PHYSICAL AGING

**D. R. Rueda, M. C. García Gutiérrez, and F. J. Baltá Calleja**
Instituto de Estructura de la Materia, CSIC, Madrid, Spain

**S. Piccarolo**
Dipartimento di Ingegneria Chimica dei Processi e dei Materiali, Univeristà di Palermo, Viale delle Scienze, Palermo, Italy

*The internal order in the amorphous state of poly(ethylene terephthalate) (PET), prepared either by rapid cooling from the melt or by thermal annealing of melt pressed films above $T_g$, has been studied using the microhardness technique. The hardness increase contribution due to physical aging, as well as the influence of the cooling rate on the hardness values of the glassy samples are independently discussed. The rate of creep under the indenter (creep constant) for these materials has been also investigated. It is found that the largest value for the creep constant corresponds to the highest cooling rate of the rapidly quenched samples (7500°C/s), and to the starting melt pressed films. In addition, results reveal that the samples, showing the lowest degree of chain ordering, contain the lowest density of "embryonic" or "ordered" nano-regions; the latter controlling the viscoelastic behavior, as well as the induction time for cold crystallization. The isothermal crystallization of amorphous samples with different degree of internal order, studied by calorimetry, and the hardness increase occurring during the induction period prior to crystallization, are also comparatively discussed.*

*Keywords*: amorphous PET, internal order, microhardness, creep behavior, physical aging

Received 22 June 2000; in final form 24 June 2000.
Grateful acknowledgment is due to DGICYT, Spain (Grant PB94-0049) for the generous support of this investigation. One of us (S.P.) also acknowledges the financial support obtained from the Italian Ministry of Universities. We are indebted to Dr. Shaul M. Aharoni for his helpful comments and suggestions.
Since the paper has been submitted, Dr. S. Aharoni has drawn our attention about the following fact: the idea of nano-size regions of higher order existing in amorphous PET was initiated by Prof. Phil Geil and his students 25 years ago [19]. Yeh's examination of the morphology and properties of amorphous PET and the effect thereon of crystallization and deformation revealed the occurrence of a nodular structure observed by surface shadowing, the nodules being of the order of 7–8 nm in diameter [19]. After Geil, the idea was taken up by Harget and Siegmann [20] and by Harget and Aharoni [21].
Address correspondence to F. J. Baltá Calleja, Instituto de Estructura de la Materia, CSIC, Serrano 119, 28006 Madrid, Spain.

## INTRODUCTION

One of the areas of soft condensed matter that has stimulated much interest in the last decade has been the study of 'order' [1] and order development in the amorphous state of polymers [2]. Polymers glasses are capable to crystallize partially depending on their chain flexibility. However, it is not yet clear the exact way in which local orientational order in the amorphous material depends on chain stiffness [1]. The crystallization behavior of amorphous polymers upon thermal treatment, at temperatures above $T_g$, has been extensively investigated [3, 4]. More recently, special attention has been devoted to study the occurrence of density fluctuations as pre-crystallization states or "embryos" prior to the development of wide angle X-ray diffraction from crystals [5–8]. As a part of a wider structural study on cold crystallization of aromatic polyesters, we have investigated the crystallization kinetics of different amorphous poly(ethylene terephthalate) (PET) samples prepared by thermal treatment of a melt pressed film at temperatures near, above $T_g$ [9]. We have also examined the influence of physical aging of amorphous PEN on the hardness variation for samples thermally treated below $T_g$ [10].

Furthermore, we have recently reported new results on the structure development in PET by solidification of the molten state using very large cooling rate values [11]. Here, it was shown that the use of cooling rates larger than 5°C/s leads to amorphous materials. These amorphous samples show, however, a gradient in properties, like hardness, density and excess of small angle X-ray scattering, which suggest the occurrence of a wide spectrum of internal order for the amorphous state of PET.

The aim of the present study is to complement the above investigations on amorphous PET samples [9, 11] highlighting the influence of the internal order of the amorphous state on: (a) the hardness variation due to physical aging and (b) the creep behavior of the amorphous samples. The measurement of the creep behavior studied by microhardness is shown to be a good testing method for the characterization of the internal order of the amorphous state.

## EXPERIMENTAL

### Materials

The amorphous PET samples investigated here were described in Refs. [9 and 11]. The first set of samples was obtained by solidification of the molten state at different cooling rates (to be denoted as samples **q**) in the range of 7500°C/s (sample **q1**) down to 17°C/s (sample **q7**) [11], following the procedure of Piccarolo and coworkers [12–14] (Tab. 1). The second set of amorphous samples are melt pressed films, (denoted as samples **a**) without nucleating agent supplied by Kalle, A. G., Germany. Two further

Downloaded At: 09:52 19 January 2011

**TABLE 1** Density and microhardness of PET solidified from the melt at different cooling rates

| *Sample* | $^{\circ}C/s$ | $\rho_{aged}$ $(g/cm^3)$ | $H_{aged}$ $(MPa)$ |
|---|---|---|---|
| **q1** | 7500 | 1.3392 | 129 |
| **q2** | 700 | 1.3389 | 132 |
| **q3** | 178 | 1.3394 | 136 |
| **q4** | 88.5 | 1.3406 | 140 |
| **q5** | 76.3 | 1.3408 | 143 |
| **q6** | 18.7 | 1.3416 | 149 |
| **q7** | 17.0 | 1.3410 | 143 |

amorphous samples were prepared by thermal treatment of the original sample (**a0**) at 95°C: the first one was treated for 1.5 h (sample **a1**) and the second one was treated for 5 h (sample **a2**), both at the above temperature.

Downloaded At: 09:52 19 January 2011

## Techniques

Microhardness $H$, was measured at room temperature using a Leitz "Durimeter" tester with a Vickers square pyramidal diamond indenter. The $H$ value (in MPa) was derived from the residual area of impression using the equation $H = Kp/d^2$, where $d$ is the mean diagonal length of the indentation in m, $p$ is the applied force in N and $K$ is a geometrical factor equal to 1.854 (15). Loads of 0.10, 0.15 and 0.25 N to correct for the instant elastic recovery were used. The force was applied at a controlled rate, held for 0.1 min and removed. The length of the impression is measured to $\pm 0.5\,\mu m$. For the creep measurements under the indenter different loading times from 0.1 up to 100 min were used.

A Seifert XRD3000 $\theta/\theta$ diffractometer using Ni-filtered Cu $K_\alpha$ radiation and a scanning speed of about 1° $(2\theta)$/min was used for samples characterization. X-ray diffractograms in the interval $5-40$ $2\theta$ were recorded to determine the crystallinity index of the sample **a0**, treated at 95°C for consecutive periods of time, by means of a fit curve program.

A Perkin Elmer DSC-7 calorimeter was used to perform isothermal crystallization of samples **q1** and **q7** at 117°C under a constant nitrogen flow. The crystallization temperature of the sample was reached at a heating rate of 100°C/min. Samples of $5-8$ mg were used.

# RESULTS

## Hardening Induced by Physical Aging

Table 1 collects the values of hardness and density for the PET samples quenched from the melt at different cooling rates. In a preceding paper we discussed the variation in hardness for these amorphous PET samples depending on the cooling conditions [11]. The hardness difference between

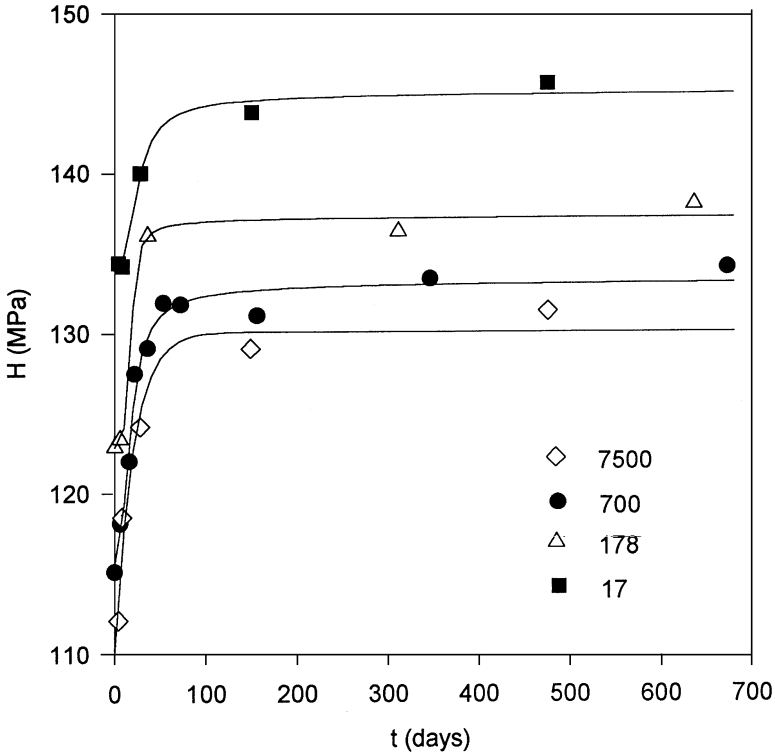


**FIGURE 1** Hardness variation with storage time of amorphous PET samples prepared at different cooling rates (in °C/s) from the molten state.

Downloaded At: 09:52 19 January 2011

the stored samples (after 40 days storage) and the "rejuvenated" samples was attributed to a physical aging of the former samples [11]. Figure 1 shows the variation of $H$ as a function of storage time for PET quenched at four selected cooling rates. A rapid increase of $H$ is observed for all the samples during the first month of storage. Thereafter, a small increase of $H$ with time takes place. The aging induced hardening effect of the samples ranges from a 15% (sample **q1**) down to a 6% (sample **q7**). What is more interesting is that the final $H$ values depend on the initial cooling rate used for the preparation of the samples. This finding favors the concept of a different state of internal order for the amorphous samples investigated.

## Creep Behavior of Amorphous PET

Owing to the apparent sensitivity of the microhardness technique to detect amorphous structures with different internal order we also measured the

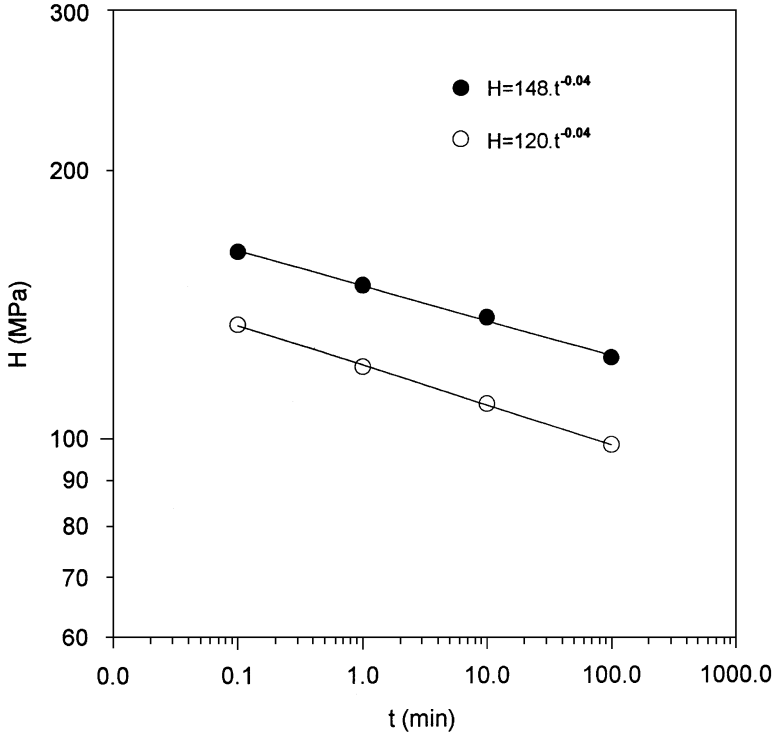


**FIGURE 2** Log–log plot of the hardness variation as a function of loading time for an amorphous PET sample (**q7**), before (full symbols) and after (open symbols) "rejuvenation". The fitted analytical expressions obtained are indicated.

creep behavior of these samples under the indenter by loading the samples for different time intervals. Figure 2 shows the log–log plot of microhardness as a function of loading time for sample **q7**, before (full symbols) and after its "rejuvenation" (open symbols) upon annealing at 95°C for 2 minutes [11, 16]. Hardness follows a variation of the type $H = H_o\, t^{-k}$ where $H_o$ is a constant and $k$ is the so-called creep constant [17]. Nearly the same creep constant value is found for sample **q7**, before and after rejuvenation, *i.e.*, the creep constant seems not to be affected by the physical aging of the amorphous state of PET. A similar finding has been previously reported for PET free of nucleating agents [18]. However, we also found that physical aging may reduce the rate of creep when PET contains chemical nucleants [18].

The creep behavior of two samples with different cooling rates (**q1** and **q7**) is presented in Figure 3. In this case, the slope (rate of creep) is clearly different for the two samples investigated, the highest rate of creep ($k = 0.08$)

Downloaded At: 09:52 19 January 2011

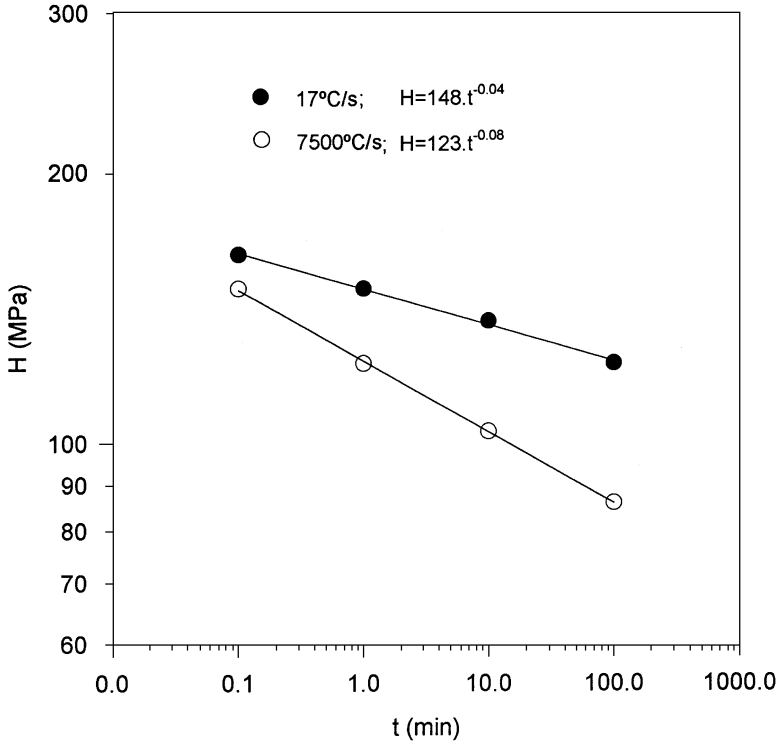


**FIGURE 3** Log–log plot of the hardness variation as a function of loading time for two amorphous PET samples solidified at different cooling rates.

Downloaded At: 09:52 19 January 2011

corresponding to sample **q1**. In addition, Figure 4 shows the creep behavior obtained for the melt pressed amorphous samples **a0**, **a1** and **a2**. In this case the rate of creep is highest for the untreated sample, **a0**, and it decreases from sample **a1** to sample **a2**, *i.e.*, the rate of creep (creep constant) decreases with increasing treatment time of PET at 95°C. In this case the creep constant variation lies within the range observed for samples **q1** and **q7** (Fig. 3). In particular, the rate of creep for sample **a0** ($k = 0.08$) is similar to that of sample **q1**.

## Degree of Order and Crystallization Behavior of Amorphous PET

Preceding '*in situ*' isothermal cold crystallization experiments by means of microhardness and X-ray scattering techniques using synchrotron radiation reveal that the various amorphous samples exhibit different crystallization kinetics parameters (induction time, $t_{ind}$) [9, 11]. In the present study we

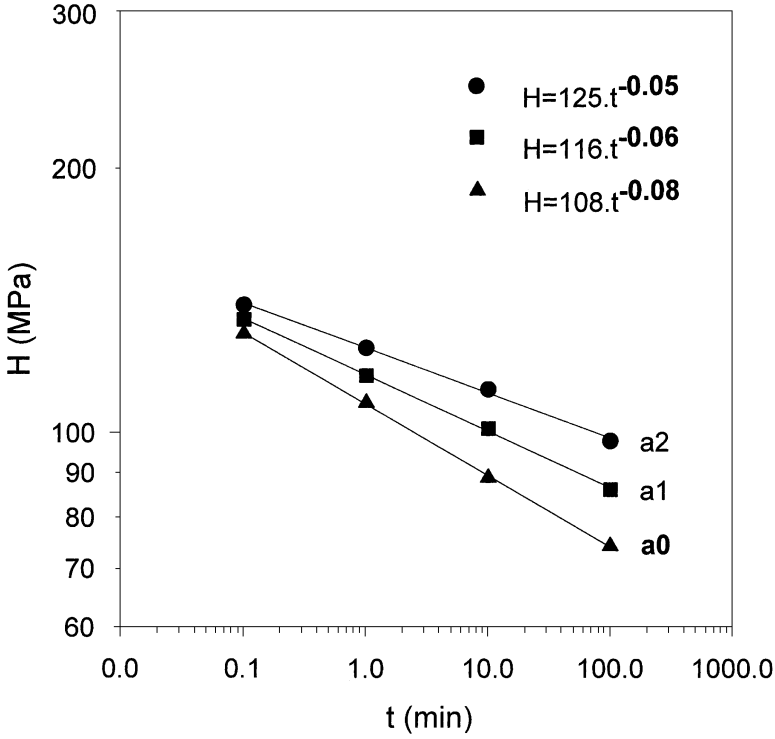


**FIGURE 4** Log–log plot of the $H$ variation *vs.* loading time for the amorphous PET samples **a0**, **a1**, and **a2** (for details see experimental part).

Downloaded At: 09:52 19 January 2011

bring additional results which allow one to examine the influence of the structure of amorphous PET on its crystallization behavior as revealed by calorimetry, microhardness and X-ray diffraction measurements.

(1) *Cold crystallization studied by DSC* Figure 5 illustrates the exothermic curves corresponding to the isothermal crystallization at 117°C for the amorphous samples **q1** and **q7**, respectively. The shape of the curves is quite different from each other, indicating the occurrence of a different crystallization kinetics for the two samples. The fraction of crystallized material as a function of time has been calculated from these curves (Fig. 6). While sample **q7** starts to crystallize sooner the crystallization of sample **q1** is delayed for about 6 min. Nevertheless, after this initial induction time sample **q1** crystallizes more rapidly than sample **q7**.

(2) *Stepwise cold crystallization studied by microhardness and X-ray diffraction* Since the samples **a1** and **a2** were prepared after heat treatment of sample **a0** at 95°C, we have next followed the cold crystallization of sample **a0**, "*in situ*", at this temperature. For this purpose the same piece

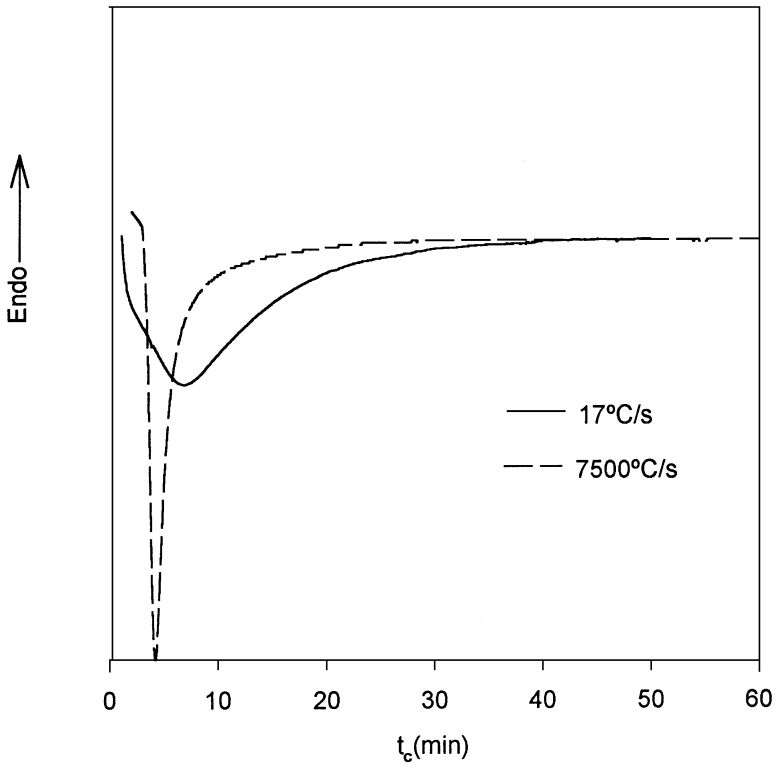


**FIGURE 5** DSC isothermal crystallization curves obtained at $T_c = 117°C$ for two amorphous PET samples with different cooling rates: **q1** (dotted curve); **q7** (continuous curve).

of sample **a0** was used to carry out the consecutive thermal treatments followed by the hardness and X-ray diffraction study at room temperature. The concurrent variation of $H$ and X-ray crystallinity ($X_c$) as a function of the crystallization time is shown in Figure 7 top-bottom, respectively. While no variation of $X_c$ after the first 7 h of treatment of PET at 95°C is observed (Fig. 7 bottom), a gradual increase of $H$ in this interval is detected. After the induction period prior to crystallization ($t_{ind} \sim 8$ h), $X_c$ rapidly increases with $t_c$ up to about $t_c = 18$ h (primary crystallization). Thereafter, $X_c$ increases more slowly (secondary crystallization). The $X_c$ rapid variation from 0 (for $t_c = 8$ h) up to 15% (for $t_c = 18$ h) is accompanied by a faster hardening of the sample in comparison to the hardness increase observed during the induction time. The final maximum value of $X_c$ is relatively low ($X_c \sim 17\%$) because of the low crystallization temperature used.

Downloaded At: 09:52 19 January 2011

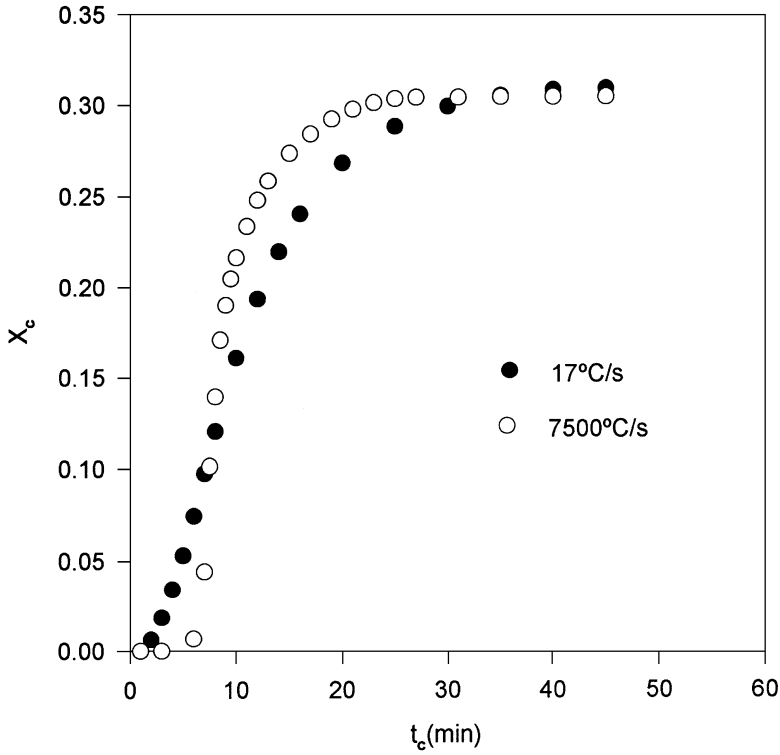


**FIGURE 6** Variation of the degree of crystallinity derived from the two DSC curves (exotherms) of Figure 5 as a function of crystallization time at $T_c = 117°C$.

Downloaded At: 09:52 19 January 2011

## DISCUSSION

In agreement with previous findings [9, 11], the above results evidence that a wide range of "structures" with different internal order can develop in amorphous PET. The generation of a varying degree of order in the amorphous state can be produced either: (a) by rapid cooling from the melt or (b) by heating amorphous PET at temperatures $T_c$ slightly above $T_g$ for times $t < t_{ind}$ at $T_c$. The results of Figure 1 reveal that for the samples stored at room temperature most of the hardening (physical aging) takes place during the first month after their preparation (or their "rejuvenation"). The relative hardening is larger for those amorphous samples that show a lower degree of internal order. Let us consider the small angle X-ray scattering intensity observed for samples **q1** and **q7** (samples defining the internal order spectrum of the amorphous state) [11]. The scattering intensity of sample **q7** is higher than that of sample **q1**. Consequently, one might expect that

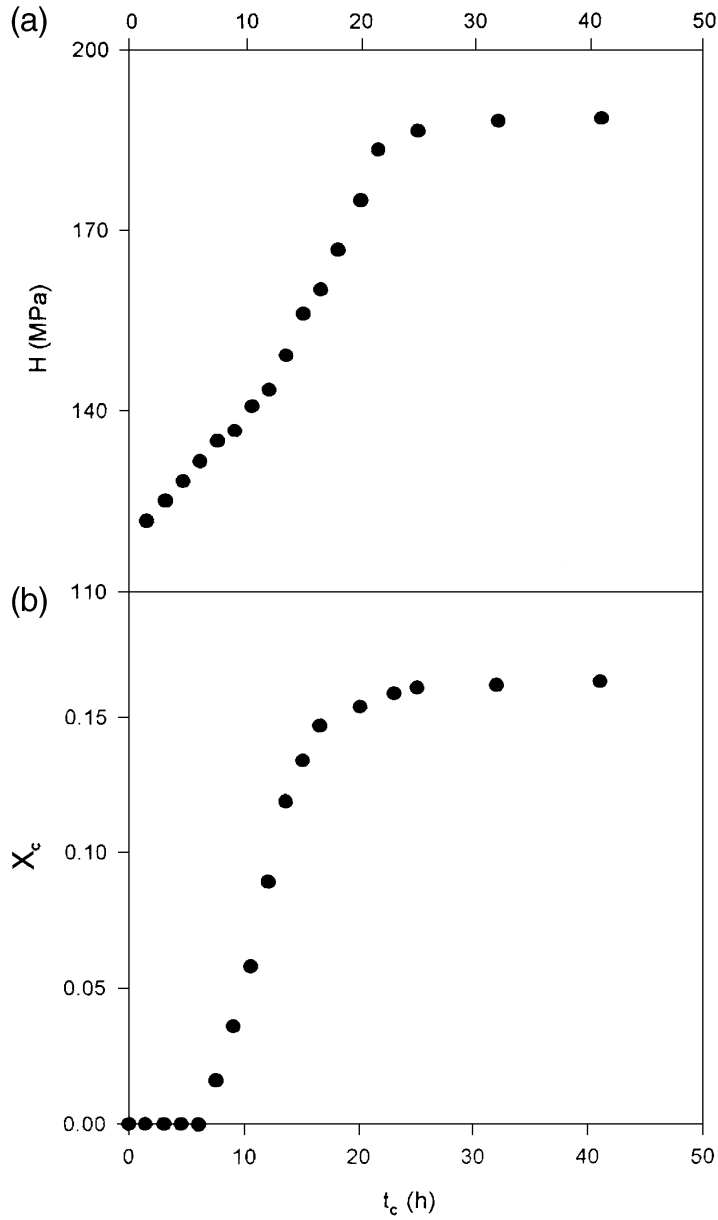


**FIGURE 7** (a): Stepwise hardness variation as a function of crystallization time at $T_c = 95°C$ measured at room temperature, for melt pressed PET film (sample **a0**); (b): Concurrent variation of the crystallinity index measured at room temperature on the same PET sample.

Downloaded At: 09:52 19 January 2011

sample **q7** should contain a higher level of electron density fluctuations ("embryonic" precrystallization states). In other words, sample **q7** should be more 'structured' (higher degree of internal order) than sample **q1**. Following the same reasoning one could speculate that the degree of internal order increases when going from sample **a0** to sample **a2**. Furthermore, we have previously observed that the initial long period appearing at a given crystallization temperature $T_c$ is larger for the amorphous samples (**q1** and **a0**) with a lower degree of internal order. This result suggests that sample **q1** exhibits a smaller concentration of larger electron density fluctuations in the 10 nm scale than sample **q7**. Most revealing is the explanation of the above results in the light of the creep behavior. Indeed, the creep constant observed for sample **q1** and sample **a0** is larger than the creep constant for samples **q7** and **a2** (Figs. 3 and 4). In other words the creep behavior of amorphous PET is considerably reduced by the presence of "ordered" nanoregions that may play the role of "embryos" or nuclei of precrystallization.

Comparison of the calorimetric results obtained for samples **q1** and **q7** (Figs. 5 and 6) emphasizes the role of the amorphous structure (showing the occurrence of ordered nanoregions) on the crystallization kinetics. Thus, the beginning of the crystallization process in sample **q1** is delayed by about 6 min in relation to sample **q7**, owing to the fact that sample **q1** is less rich in "ordered" nanoregions than sample **q7**. In addition, from Figure 6 and from the data previously reported for samples **a0**, **a1** and **a2** in Ref. [9], it appears that the crystallization kinetics is also affected by the way the amorphous structure have developed. Thus, in the case of samples **a0**, **a1** and **a2** the reported crystallization kinetics curves regarding crystallinity and SAXS invariant [9], are parallel to each other in contrast to the crystallinity results obtained for samples **q1** and **q7** (Fig. 6), which show a cross-over at $t_c = 9$ min.

In summary, the microhardness has been shown to be a technique that is able to reveal changes of internal order in the amorphous state. Indeed, it is remarkable the hardening observed during the first 7 h of treatment at 95°C of sample **a0** (Fig. 7 top) while no X-ray diffraction from crystals is detected in the same period of time (Fig. 7 bottom). Comparison of microhardness and the wide-angle X-ray scattering appears to be an excellent means of analysis of cold crystallization measurements, particularly when low $T_c$ values are used.

## CONCLUSIONS

(1) The creep constant values for the amorphous PET samples investigated, as derived from microhardness measurements, range between 0.04 and 0.08. The lower values of the creep constant can be associated to the amorphous material with a higher degree of internal order, *i.e.*, containing a higher level of "embryonic" ordered nanoregions.

Downloaded At: 09:52 19 January 2011

(2) Physical aging upon storage of amorphous PET is contributing to a maximum hardness increase of about 15%. Most of this hardening occurs during the first month, after preparation or after rejuvenation of the amorphous sample.
(3) The hardness of aged amorphous PET is higher the internal order of the starting material.

## REFERENCES

[1] Keinath, S. E., Miller, R. L. and Rieke, J. K. Eds. (1987). *Order in the Amorphous State of Polymers*, Plenum Press, New York.
[2] Keller, A., Warner, M. and Windle, A. H. Eds. (1999). *Self Order and Form in Polymeric Materials*, Chapman & Hall, London.
[3] Baltá Calleja, F. J. and Ezquerra, T. A., "Polymer Crystallization General Concepts of Theory and Experiments", In: *Encyclopedia of Materials*: *Science and Technology*, Elsevier, Oxford (in press).
[4] Zachmann, H. G. and Wutz, C. (1993). *Crystallization of Polymers* (Ed. Dosière, M.), Kluver Academic Press, Dordrecht.
[5] Imai, M., Mori, K., Mizukami, T., Kaji, K. and Kanaya, T. (1992). *Polymer*, **33**, 4451.
[6] Imai, M., Kaji, K., Kanaya, T. and Sakai, Y. (1995). *Phys. Rev. B*, **52**, 1.
[7] Ezquerra, T. A., López-Cabarcos, E., Hsiao, B. H. and Baltá Calleja, F. J. (1996). *Phys. Rev. E*, **54**, 989.
[8] Ania, F., Cagiao, M. E. and Baltá Calleja, F. J. (1999). *Polymer J.*, **31**(9), 735.
[9] García Gutiérrez, M. C., Rueda, D. R. and Baltá Calleja, F. J. (1999). *Polymer J.*, **31**, 806.
[10] Rueda, D. R., Varkalis, A., Viksne, A., Baltá Calleja, F. J. and Zachmann, H. G. (1995). *J. Polym. Sci.*, **B33**, 1653.
[11] Baltá Calleja, F. J., García Gutiérrez, M. C., Rueda, D. R. and Piccarolo, S. (2000). *Polymer*, **41**, 4143.
[12] Brucato, V., Crippa, G., Piccarolo, S. and Titomanlio, G. (1991). *Polym. Eng. Sci.*, **31**, 1411.
[13] Piccarolo, S., Saiu, M., Brucato, V. and Titomanlio, G. (1992). *Appl. Polym. Sci.*, **46**, 625.
[14] Piccarolo, S. (1992). *J. Macromol. Sci.-Phys.*, **B31**(4), 501.
[15] Baltá Calleja, F. J. (1994). *Trends Polym. Sci.*, **2**, 419.
[16] Struik, L. C. E. (1978). *Physical Aging in Amorphous Polymers and other Materials*, Elsevier, Amsterdam.
[17] Baltá Calleja, F. J. (1985). *Adv. Polym. Sci.*, **66**, 177.
[18] Baltá Calleja, F. J., Santa Cruz, C. and Asano, T. (1993). *J. Polym. Sci.*, **B31**, 557.
[19] Yeh, G. S. Y. and Geil, P. M. (1967). *J. Macromol. Sci.-Phys.*, **B1**(2), 237.
[20] Harget, P. J. and Siegmann, A. (1972). *J. Appl. Phys.*, **43**, 4357.
[21] Harget, P. J. and Aharoni, S. M. (1976). *J. Macromol. Sci.-Phys.*, **B12**, 209.

Downloaded At: 09:52 19 January 2011